Distributed Auxiliary Inverter of Urban Rail Train—Load Sharing Control Strategy Under Complicated Operation Condition

Jie Chen, Lei Wang, Lijun Diao, *Member, IEEE*, Huiqing Du, and Zhigang Liu

***Abstract*—Paralleling is the development tendency of the auxiliary inverter. This paper analyzes the problems of the parallel process in detail. First, for inherent contraction between voltage regulation performance and current sharing performance, the paper adopts the resistive droop method. Second, the paper improves dynamic performance and reliability of the droop method by improving power calculation and introducing the whole cycle adaptive droop method. Third, in order to solve the unshared current problem caused by inconsistent parameters, the paper increases active power proportion droop coefficient, and introduces voltage compensation strategy to compensate voltage drop caused by increased proportion droop coefficient. Fourth, the auxiliary parallel system has complicated load characteristics; the paper proposes voltage compensation strategy to compensate voltage drop caused by the pump load. This paper utilizes three-phase total reactive power to droop frequency and active power of each phase to droop amplitude, unbalanced current can be shared. This paper introduces special virtual impedance technology to solve the harmonic current sharing problem caused by the nonlinear load. Finally, the effectiveness of above theory is fully verified by simulation and experiment.**

***Index Terms*—Droop method, parallel inverter, resonant controller, virtual impedance, voltage compensation strategy.**

I. Introduction

With the swift and violent development of China's urban rail transit, the advanced requirement about the auxiliary inverter of the urban rail train is proposed, except for promoting the performance of the single inverter, the most effective way about improving performance of the auxiliary system is parallel. The auxiliary system power supply in parallel can solve the drawbacks of crossing supply or extending supply, and can promote reliability and redundancy of the whole system.

The parallel methods include centralized control [1], master–slave control [2], 3C control [3], wired distributed control [4], and wireless parallel control [5], etc. However, except for wireless parallel control, coupling exists in the other methods and the inverter is not completely independent individual. Therefore, the paper adopts wireless parallel technique.

Wireless parallel technique generally adopts the droop method [6], [7], the traditional droop method derives from grid connection technology of the synchronous generator [8], which is based on inductive system impedance [9], and adopts active power to drop frequency and reactive power to drop amplitude [10]. Although the droop method which makes the wireless parallel system have power sharing capability, there are still some shortcomings.

1) For the limit of frequency and amplitude range, the proportion droop coefficient has to be small especially under large-load condition, which goes against power sharing. If the droop coefficient is enlarged to improve power sharing performance, it would make output voltage deviate from rated value. Therefore, it is an inherent contradiction between voltage regulation performance and power sharing performance.
2) Dynamic performance of the droop method is poor, it is easy to generate oscillation especially in the instant when the new inverter is added. The paper [11] introduces derivative control into the droop method, which can respond to variation of power and promote dynamic performance greatly. However, derivative control also introduces high-frequency disturbance and decreases stability, especially when the parallel system operates under no-load condition.
3) Because the parameters of every inverter in the parallel system are impossible to be consistent, inconsistent circuit parameters and AD sampling parameters make the parallel system output unshared current, the wireless droop method is difficult to suppress the effect of inconsistent parameters.
4) The auxiliary system has complex load condition. The surge current caused by pump load makes frequency and amplitude deviate from rated value under the droop method. Unbalanced load and nonlinear load give rise to unbalanced current and harmonic current, which are difficult to be shared by the droop method.

This paper aims at overcoming above shortcomings, and focus on resolving the last problems mainly. This paper adopts the resistive droop method (RDM), which can better improve inherent contradiction, guarantee the voltage regulation and power sharing performance; for improving the dynamic performance, this paper improves the power calculation method to decrease

Manuscript received October 24, 2014; revised December 12, 2014 and March 15, 2015; accepted April 14, 2015. Date of publication April 28, 2015; date of current version November 16, 2015. This work was supported by the China National Key Technologies R&D Program under Grants 2013BAG24B01 and 2013BAG21Q00. Recommended for publication by Associate Editor D. Vinnikov.

J. Chen is with the Department of Electrical Engineering, Laboratory for Rail Transportation Electrical Equipment, Beijing Jiaotong University, Beijing 100044, China, and also with the Institute of Electrical Engineering, Chinese Academy of Sciences, Beijing 100190, China (e-mail: wcchenjie@gmail.com).

L. Wang, L. Diao, H. Du, and Z. Liu are with the Department of Electrical Engineering, Laboratory for Rail Transportation Electrical Equipment, Beijing Jiaotong University, Beijing 100044, China (e-mail: leiwang@bjtu.edu.cn; ljdiao@bjtu.edu.cn; 11117361@bjtu.edu.cn; zhgliu@bjtu.edu.cn).

Digital Object Identifier 10.1109/TPEL.2015.2427381

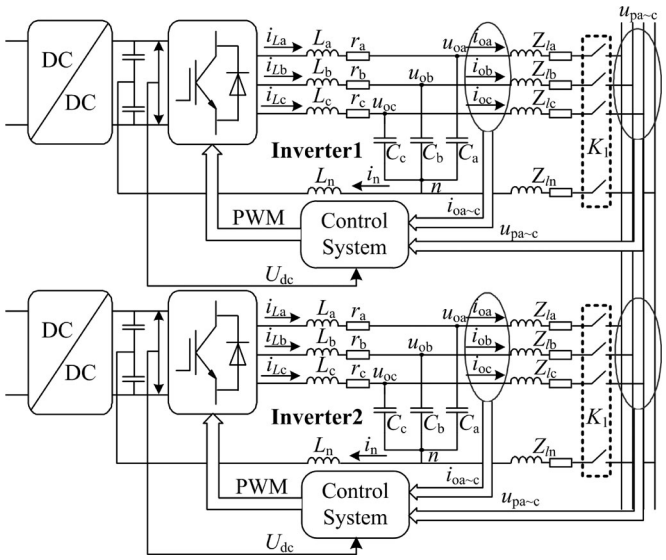

Fig. 1. Topology of a parallel auxiliary system.

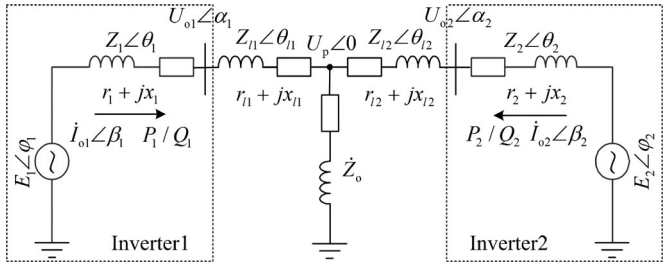

Fig. 2. Model of a parallel inverter.

the delay time of power calculation, and proposes the whole cycle adaptive droop method (TWCADM) to improve dynamic performance and guarantee system stability. In order to solve the problem of the unshared current caused by inconsistent parameters, this paper enlarges the proportion droop coefficient to improve power sharing performance. However, increased proportion droop coefficient will decrease the amplitude of the output voltage greatly. In order to compensate the voltage drop, this paper proposes the voltage compensation strategy, which can recover the output voltage dynamically; the auxiliary system has complicated load condition. This paper proposes the voltage compensation strategy to compensate the voltage drop caused by the pump load, independent active power droop and uniform reactive power droop to solve the problem of unbalanced load, and especial virtual impedance technology to share harmonic current caused by the nonlinear load. Based on the above methods, the output current can be shared under complicated load condition.

II. Resistive Droop Method

The topology of the parallel auxiliary system is shown in Fig. 1, the converter is cascaded dc/dc with the inverter, the dc-link voltage of inverter is mainly decided by dc/dc. The control system needs to sample the bus voltage ($u_{\mathrm{pa}\sim c}$), output current ($i_{\mathrm{oa}\sim c}$), and dc-link voltage (U_{dc}). In Fig. 1, there are only two parallel inverter, but the number of inverters exceeds two is also permitted.

An inverter is an adjustable voltage source with internal impedance in essence [12], therefore, the model of the parallel system can be established, as shown in Fig. 2. $Z_{\mathrm{li}}\angle\theta_{\mathrm{li}}$ is the parasitic impedance of line, $E_i\angle\varphi_i$ is the no-load voltage of the inverter, $Z_i\angle\theta_i$ is the internal impedance of the inverter, $U_{\mathrm{oi}}\angle\alpha_i$ is the output voltage of the inverter (*i* is ID number of the inverter), Z_{o} is load of the parallel system, and $U_p\angle 0$ is the bus voltage. The system impedance can be given as

$$Z_{\mathrm{si}}\angle\theta_{\mathrm{si}} = Z_i\angle\theta_i + Z_{\mathrm{li}}\angle\theta_{\mathrm{li}}. \tag{1}$$

If the system impedance is inductive ($\theta_{\mathrm{si}} = 90^\circ$), the inductive droop method (IDM, traditional method) can be obtained

$$\begin{aligned} \omega_{\mathrm{ref}} &= \omega_0 - mP \\ E_{\mathrm{ref}} &= E_0 - nQ. \end{aligned} \tag{2}$$

If the system impedance is resistive ($\theta_{\mathrm{si}} = 0^\circ$), the RDM can be obtained

$$\begin{aligned} E_{\mathrm{ref}} &= E_0 - mP \\ \omega_{\mathrm{ref}} &= \omega_0 + nQ. \end{aligned} \tag{3}$$

In equation (2) and (3), E_0 and ω_0 are the voltage amplitude and frequency with no-load, E_{ref} and ω_{ref} are the voltage amplitude and frequency reference, *m* is the active power droop coefficient, and *n* is the reactive power droop coefficient.

Because the power factor of the auxiliary inverter is generally higher than 0.85; if IDM is employed, the small allowable frequency fluctuation range (± 0.5 Hz) will limit the active power droop coefficient *m* greatly; if RDM is employed, due to the smaller reactive power, the reactive power coefficient *n* can be larger. The larger droop coefficient can obtain the greater power sharing performance, therefore, RDM is a better choice and can both meet the requirements of voltage regulation performance and power sharing performance.

The foundation of the RDM is the resistive system impedance. The parasitic impedance of line $Z_{\mathrm{li}}\angle\theta_{\mathrm{li}}$ is generally resistive in medium- and low-voltage systems [13]. In addition, if the double-loop control strategy based on the modified resonant controller is employed, the internal impedance of the inverter $Z_i\angle\theta_i$ is resistive too. Therefore, the system impedance can become resistive, and the RDM can be employed.

III. Improving the Dynamic

Although the RDM improves the inherent contradiction between voltage regulation performance and power sharing performance, the dynamic performance of the RDM is still poor; there are two essential reasons, one is the application of large-delay low-pass filter (LPF), which is used in power calculation, another one is only simple proportion droop is used in the RDM, which restrict the dynamic performance of the parallel system.

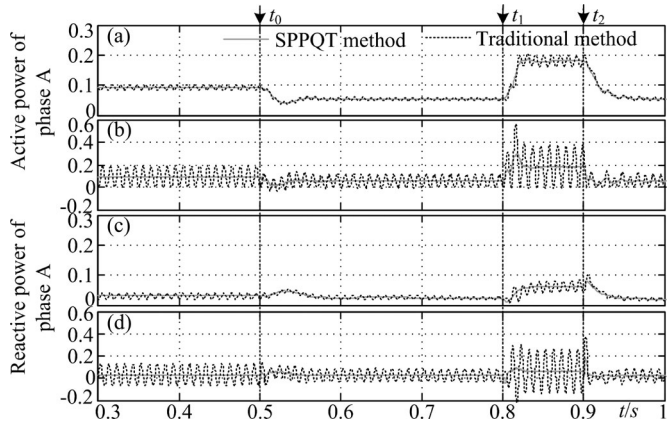

Fig. 3. Comparison of power calculation methods. (a) Active power of phase A with LPF. (b) Active power of phase A without LPF. (c) Reactive power of phase A with LPF. (d) Reactive power of phase A without LPF.

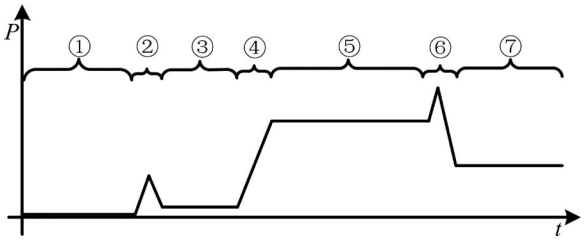

Fig. 4. Process of a parallel system.

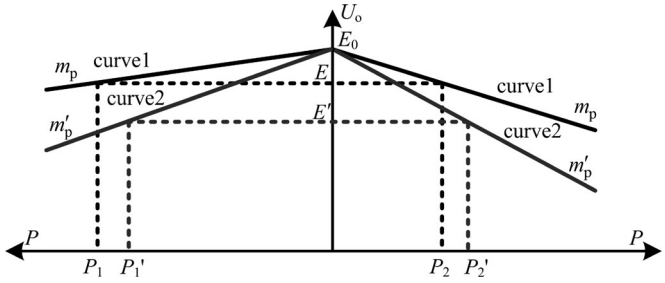

Fig. 5. Droop curve.

A. Improvement of Power Calculation

In balanced three-phase system, the three-phase power can be acquired through coordinate transformation or method of symmetrical components [14], but the way is inaccurate for calculating unbalanced and harmonic power; for more accurate control, the droop method requires different droop quantity for each phase with unbalanced load, therefore, independent power calculation [15] for each phase is the better choice.

Traditional power calculation [16] produces double-frequency ac value, which is harmful to droop control. In order to filter the ac value, the large-delay LPF has to be employed, the cutoff frequency of which must be less than one-tenth of the fundamental frequency [16]. However, the single-phase PQ theory (SPPQT) can solve the problem of the traditional method [15]

$$\begin{aligned} P &= 0.5U_pI_o + 0.5U_p(-90^\circ)I_o(-90^\circ) \\ Q &= 0.5U_p(-90^\circ)I_o - 0.5U_pI_o(-90^\circ). \end{aligned} \tag{4}$$

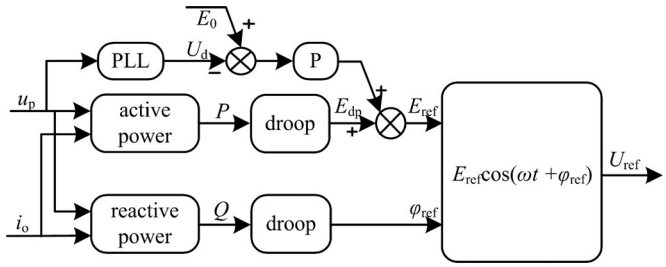

Fig. 6. Method of voltage compensation.

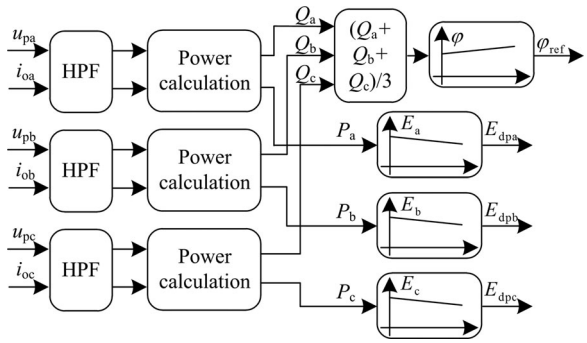

Fig. 7. Improvement of the droop method under unbalanced load.

This method can obtain the constant power directly and large-delay LPF can be omitted, small-delay LPF will be employed to filter high-frequency ripple of power, the cutoff frequency can achieve more than one-fifth of the fundamental frequency, and the dynamic performance of parallel system can be improved. However, this method needs to sample 90° delayed voltage and current, respectively, the simplest method is storing a quarter period of voltage and current in memory to read in cycle.

The comparison of power calculation methods is shown in Fig. 3. The traditional method is oscillating seriously and the SPPQT method is smooth, which decreases delay time of LPF, and even if 90° delay exists in the SPPQT method, the dynamic characteristic still can be fast. First, the cutoff frequency of the LPF used in the SPPQT method is higher than the traditional method, which means faster dynamic response. Second, there is still half-real-time voltage and current except delayed voltage and current, the transient load can still be reflected in the SPPQT method. Third, serious oscillation of the traditional method needs more time to filter in the same cutoff frequency, especially the transient load occurs in the peak value of oscillation, the details of which can be seen in t_2 of Fig 3.

B. Whole Cycle Adaptive Droop Method

Except for improving power calculation, introducing derivative control [11], [17], [18] into the droop method also can improve the dynamic performance

$$\begin{aligned} E_{\mathrm{ref}} &= E_0 - (m_p + m_d s)P \\ \varphi_{\mathrm{ref}} &= \varphi_0 + (n_p + \frac{n_{\mathrm{i}}}{s} + n_d s)Q. \end{aligned} \tag{5}$$

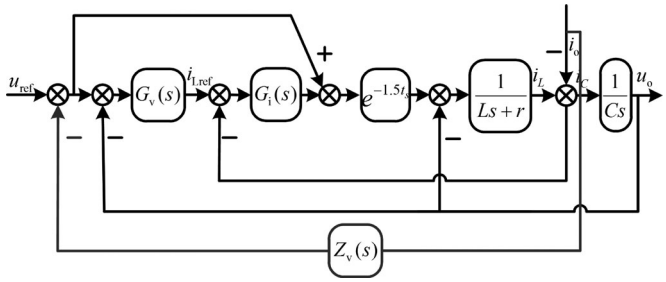

Fig. 8. Virtual impedance technology.

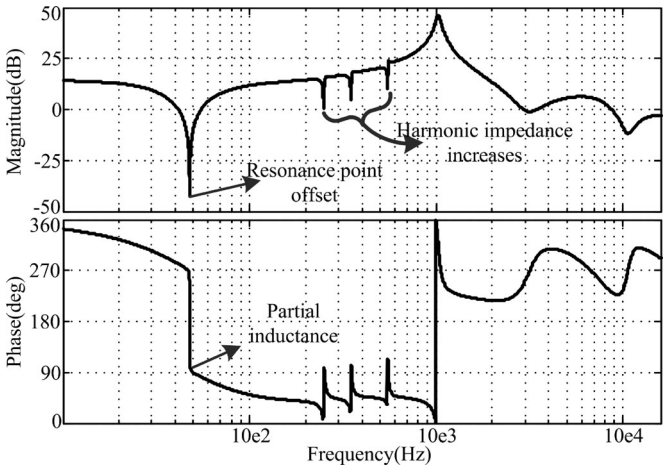

Fig. 9. Bode diagram of Zn(s) with inductive virtual impedance.

Equation (5) improves frequency droop to angle droop, the target of which is to increase differential order. The benefit of derivative control is that the droop method can respond to variation of power, which means the dynamic performance of the droop method can be improved, and will quickly respond to transient power. However, derivative control may make parallel system unstable, especially when the inverter is under no-load condition.

The power curve in the whole operation process is shown in Fig. 4, ①is the process of single inverter operating with no-load, a new inverter is added in process, ②there is power peak and becomes smooth in process, ③the parallel system is loaded in process, ④and becomes smooth in process ⑤again, the third inverter is added in process ⑥and generates power peak, finally, the power curve becomes smooth again. The whole operation process can be divided into three parts, one is process ①and ③, at these time, inverters are operating under no-load condition (stability is not good under no-load condition), especially process ③, two inverters operates under no-load condition, which requires small differential coefficient as possible. The second part is process ②④⑥, at these time, power transient requires large differential coefficient to suppress the current peak. The third part is process ⑤⑦, in these processes, inverters operate under load condition and the power curve is smooth and stable, the differential effect is not obvious, not too large differential coefficient is required to guarantee stability.

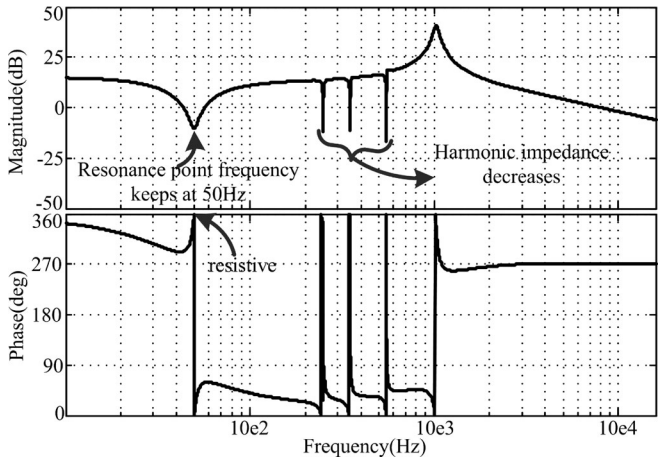

Fig. 10. Bode diagram of Zn(s) with resistive virtual impedance.

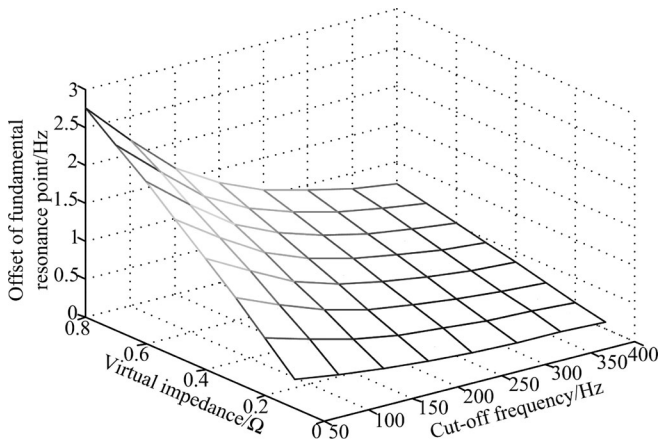

Fig. 11. Relation between resonance point offset and virtual impedance and cutoff frequency.

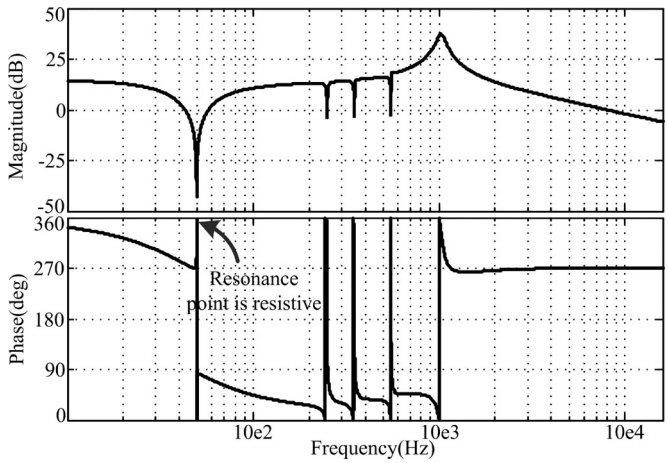

Fig. 12. Bode diagram of Zn(s) when LPF and HPF are both used.

Recorrect the differential part of the droop method, as shown in (6)

$$\begin{cases} \tilde{m}_d = \left| A_p G_{\mathrm{LPF}}(s) \dfrac{dP}{dt}(1 - B_p P) \right| m_d \\ \tilde{n}_d = \left| A_q G_{\mathrm{LPF}}(s) \dfrac{dQ}{dt}(1 - B_q Q) \right| n_d \end{cases} \tag{6}$$

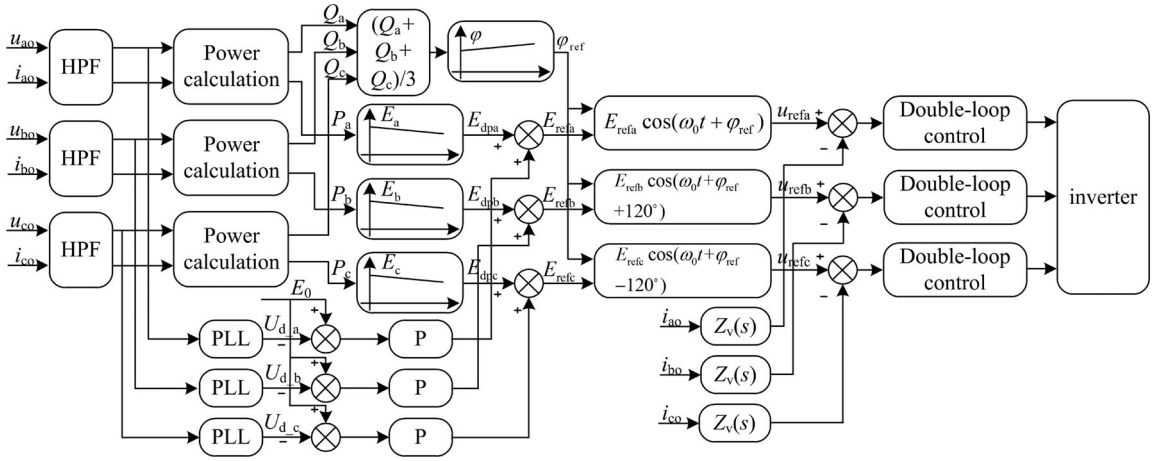

Fig. 13. Total control strategy.

where coefficient *A* is reciprocal of the maximum power in the whole operation period (A_p corresponds to active power, A_q corresponds to reactive power), coefficient *B* is reciprocal of the maximum power under no-load condition (B_p corresponds to active power, B_q corresponds to reactive power), what calls for special attention is that the effect of the circular current must be considered. $G_{\mathrm{LPF}}(s)$ is the LPF, the cutoff frequency should be 5–10 times than the cutoff frequency of the LPF used in power calculation, which can filter high-frequency disturbance introduced by power calculation and guarantee response speed of derivative control to be faster than response speed of proportional control.

TWCADM can be given finally

$$\begin{aligned} E_{\mathrm{ref}} &= E_0 - (m_p + \tilde{m}_d s)P \\ \varphi_{\mathrm{ref}} &= \varphi_0 + (n_p + \frac{n_i}{s} + \tilde{n}_d s)Q. \end{aligned} \tag{7}$$

Equation (7) takes full account of power changes that occur in the whole operation process, realizes differential coefficient adaptive adjusting in the whole operation process. Because of (1–B_pP) and (1–B_qQ), the differential coefficient can be so small that stability does not get affected when the parallel system runs under no-load condition. Because of $A_pG_{\mathrm{LPF}}(s)dP/dt$ and $A_qG_{\mathrm{LPF}}(s)dQ/dt$, the differential coefficient can be increased rapidly with power changing (coefficient *A* restricts the maximum of differential coefficient), the dynamic performance of the parallel system can be improved greatly when power transient occurs. If the parallel system operates under load condition, because *dP*/*dt* and *dQ*/*dt* are very small, differential coefficient keeps small and stability of the parallel system does not get affected. Therefore, the differential coefficient has the ability of dynamic regulation according to actual requirement, which improves the dynamic performance and guarantees stability of the parallel system as well.

IV. Parallel Strategy with Inconsistent Parameters

Inconsistent parameters are ubiquitous in practice, which means circle parameters (such as filer parameters or parasitic parameters) and sampling circle parameters have differences even if design values are consistent, the condition will result in unshared current.

According to Fig. 2, the output voltage of inverter can be expressed

$$U_{\mathrm{oi}}\angle\alpha_i = E_i\angle\varphi_i - I_{\mathrm{oi}}\angle\beta_i Z_i\angle\theta_i. \tag{8}$$

Divide both sides of (8) by $\angle\alpha_i$

$$U_{\mathrm{oi}}\angle 0 = E_i\angle(\varphi_i - \alpha_i) - I_{\mathrm{oi}}\angle(\beta_i - \alpha_i)Z_i\angle\theta_i. \tag{9}$$

Equation (9) can be simplified

$$\begin{aligned} U_{\mathrm{oi}} = {} & E_i\cos(\varphi_i - \alpha_i) - I_{\mathrm{oi}}r_i\cos(\alpha_i - \beta_i) \\ & - I_{\mathrm{oi}}x_i\sin(\alpha_i - \beta_i). \end{aligned} \tag{10}$$

Adopting the double-loop strategy based on the modified resonant controller, (11) can be realized approximately

$$\begin{cases} \varphi_i \approx \alpha_i \\ x_i \approx 0 \\ E_i \approx E_{\mathrm{ref}} \end{cases}. \tag{11}$$

According to (11), and combining with the droop method, (10) can be simplified

$$U_{\mathrm{oi}} = E_0 - \left(m_p + \tilde{m}_d s + \frac{r_i}{E_i}\right)P_i. \tag{12}$$

Derivative control can be ignored in the steady state, (12) can be simplified

$$U_{\mathrm{oi}} = E_0 - \left(m_p + \frac{r_i}{E_i}\right)P_i. \tag{13}$$

Define

$$a_i = \frac{r_i}{E_i} \tag{14}$$

where a_i is the natural droop coefficient, which collaborates with the proportion coefficient to form the overall droop coefficient of the parallel system.

TABLE I
PARAMETERS TABLE

Sampling time/s	1e-4	Filter capacitor C/μF	20
Switch frequency/Hz	5k	Neutral inductance L_n/mH	2
Filter inductance L/mH	1.5	Power/kVA	5
Parasitic resistive $r/m\Omega$	270	Rated voltage/V	220
m_p	1e-4	m_d	3250
n_i	1e-4	n_p	3250
n_d	1000	Cutoff frequency of LPF used in power calculation/Hz	10

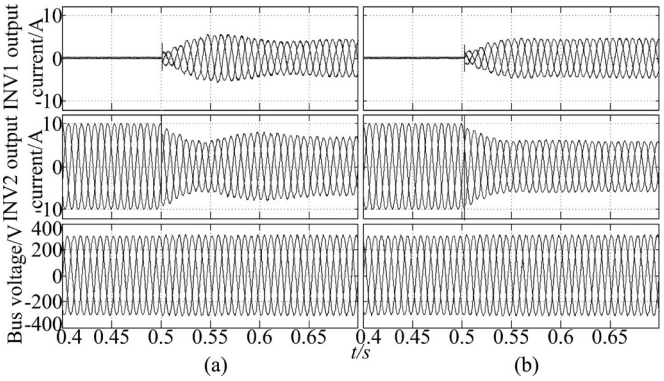

Fig. 14. Simulation result with the droop method. (a) Traditional method. (b) TWCADM.

The curve of (13) can be drawn, as shown in Fig. 5. Curve 1 is droop characteristic of the parallel system with inconsistent parameters, obviously, the slope of the left curve is less than the right curve, which means $a_1 < a_2$ and $P_1 > P_2$. Inconsistent parameters affect the droop coefficient through output impedance *r*, and then result in unshared current finally.

In order to eliminate the effect of inconsistent parameters, it is necessary to improve the droop method. As shown in curve 2 of Fig. 5, the power deviation can be balanced by means of the increasing droop coefficient m_p, although it is impossible to share power accurately, power deviation still can be reduced effectively. However, the method also has defect, as shown in curve 2, the amplitude of the output voltage falls from *E* to *E'* and deviation from rated value E_0 is further expanded.

In order to eliminate the defect introduced by the increased proportion droop coefficient, the voltage amplitude needs to be compensated. Because the droop method can regulate the amplitude in terms of load condition, the compensation method is required to eliminate the effect of load condition and have no direct connection with power or current, otherwise, the proportion droop coefficient would be reduced in disguised form.

This paper proposes the voltage amplitude compensation strategy based on phase-locked loop (PLL), as shown in Fig. 6. The voltage amplitude U_d of each phase can be obtained by PLL, comparing with no-load voltage E_0, compensation value can be acquired by P controller. The advantage of the compensation method is the compensation value that can be dynamically adjusted in terms of the voltage drop value, and the compensation value has no direct relationship with the power or current, the

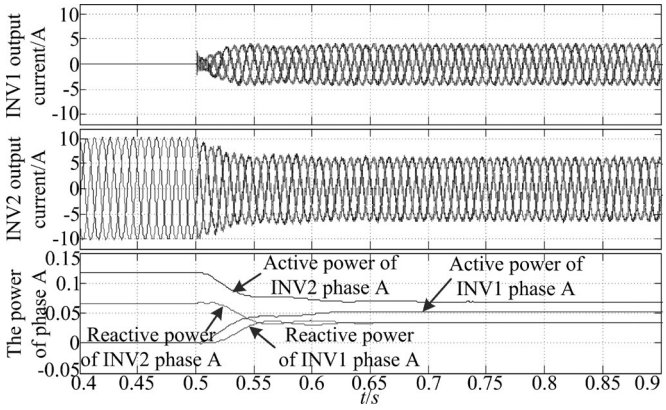

Fig. 15. Simulation result of inconsistent parameters.

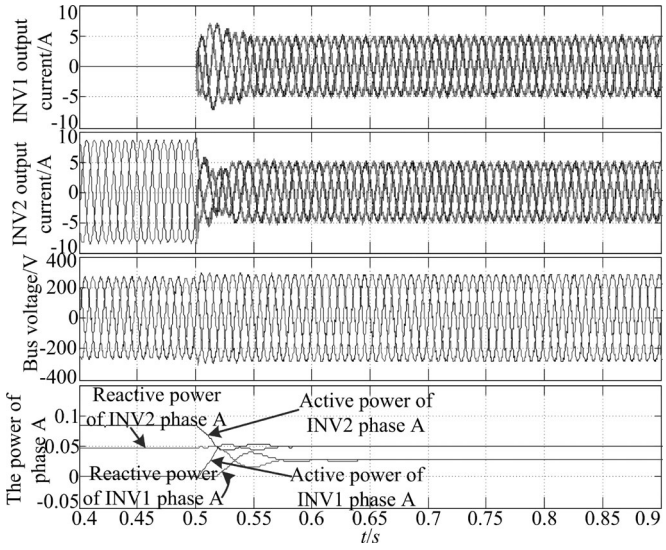

Fig. 16. Simulation result after increasing proportion coefficient with inconsistent parameters.

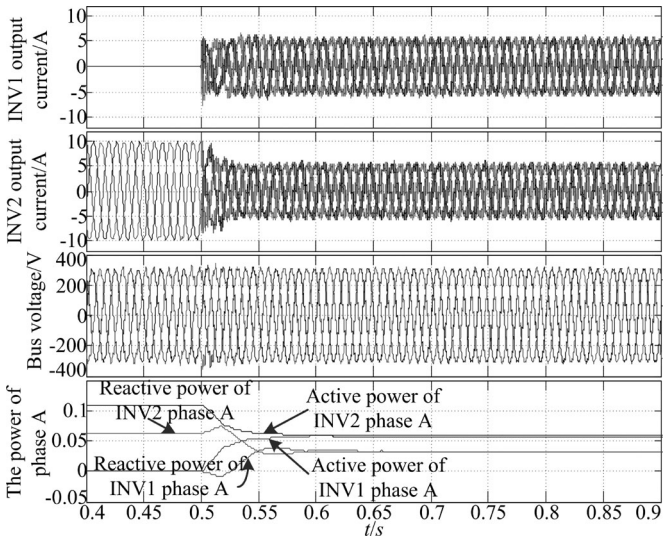

Fig. 17. Simulation result of the voltage compensation strategy.

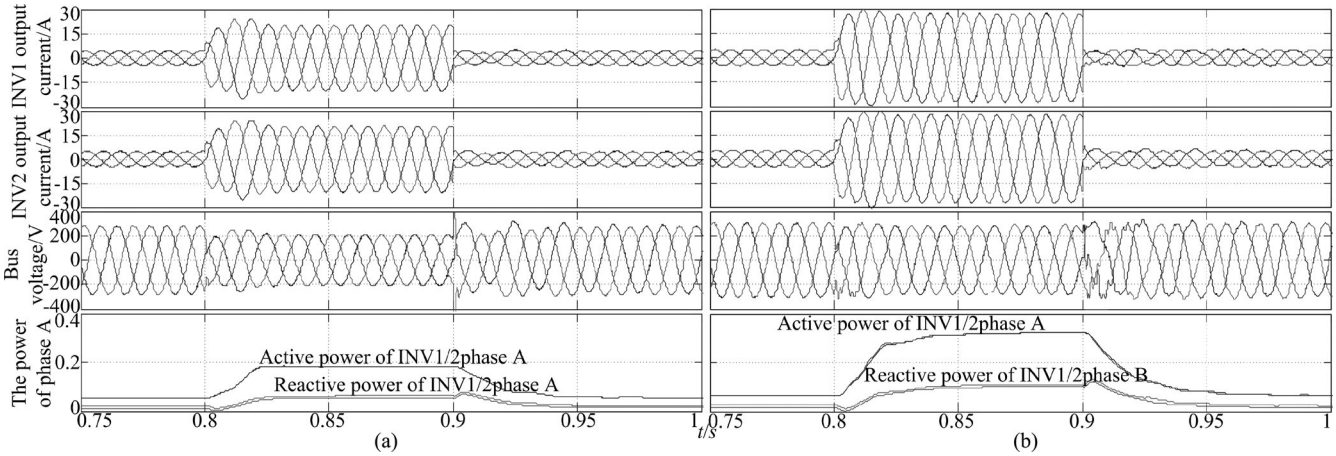

Fig. 18. Comparison of simulation result under pump load. (a) Without voltage compensation strategy. (b) With voltage compensation strategy.

proportion droop coefficient will not be affected, the objective of the recovering voltage amplitude can be achieved.

The essence of the voltage compensation method is no-load voltage E_0 of the droop method [see equation (7)] can be dynamic regulated, and the droop coefficient is not affected by compensation. If heavy load makes output voltage drop, the voltage compensation method can promote the output voltage by promoting the no-load voltage value.

V. Sharing Current Control Strategy with Complicated Load Characteristics

An auxiliary inverter has complicated load characteristics, includes pump load, unbalanced load, and nonlinear load. This section will analyze sharing current strategy with complicated load.

A. Pump Load

The characteristic of the pump load is the presence of the surge current when pump load starts, which can cause serious voltage drop, especially in the parallel system, because the surge current makes voltage further drop with the droop method. In order to solve the problem, the voltage compensation method previously mentioned can be used, the simulation and experimental results are shown in Sections VI and VII.

B. Unbalanced Load

In order to restrain the effect of the unbalanced load, the author uses the double-loop strategy based on the modified resonant controller in each phase, however, if the frequency is drooped in each phase independently, an undesirable phenomenon would appear. Reactive power droop is shown in (7), because of an integrator, the unbalanced reactive power can be accumulated and phase angle difference of each phase cannot keep 120°. In addition, even if three-phase loads are balanced, the error of power sampling still can result in the same result.

For the problem, the general method adopts three-phase total power to droop amplitude and frequency [16], but this method cannot regulate the amplitude of each phase. This paper uses the total reactive power of three-phase to droop frequency and active power of each phase to droop amplitude, which can maintain phase angle difference and regulate amplitude independently as well, as shown in Fig. 7.

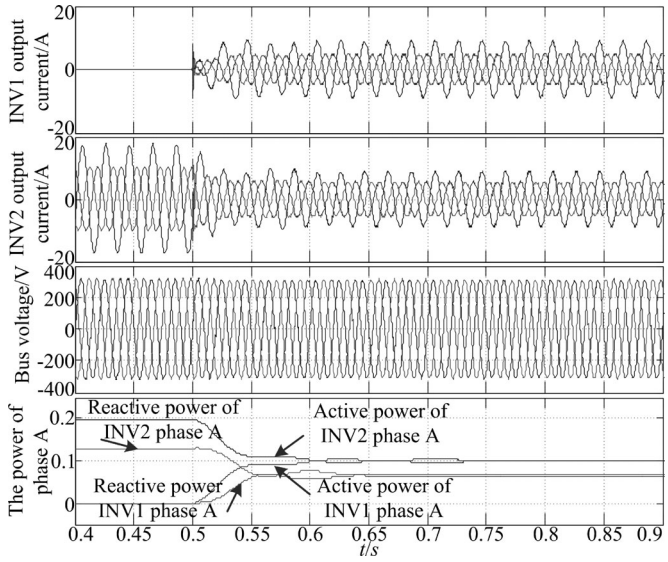

Fig. 19. Simulation result of parallel control with unbalanced load.

C. Nonlinear Load

The previously mentioned droop method can only share fundamental power, cannot share harmonic power caused by nonlinear load. In order to solve the problem, virtual impedance technology [16], [19], [20] is employed in this paper, as shown in Fig. 8.

The output voltage can be expressed on the basis of an inverter model [21]

$$u_o = G(s)u_{\text{ref}} - Z(s)i_o \tag{15}$$

where $G(s)$ is the controller and $Z(s)$ is the internal impedance. The virtual impedance can regulate internal impedance characteristic

$$u_o = G(s)u_{\text{ref}} - [G(s)Z_v(s) + Z(s)]i_o. \tag{16}$$

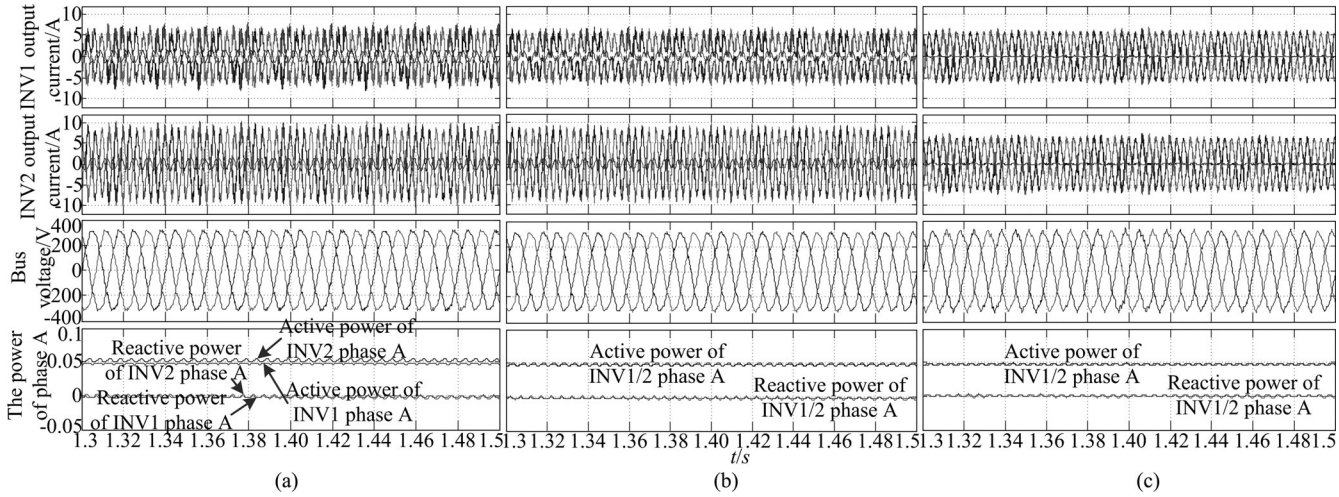

Fig. 20. Simulation result of parallel control with nonlinear load. (a) Without increasing proportion droop coefficient. (b) Increasing proportion droop coefficient. (c) Introducing virtual impedance technology.

Define

$$Z_n(s) = G(s)Z_v(s) + Z(s). \tag{17}$$

The expression of $Z_n(s)$ is as follows:

$$Z_n(s) = \frac{[G_v(s)G_i(s)+1]e^{-1.5\mathrm{st}_s}Z_v(s) + G_i(s)e^{-1.5\mathrm{st}_s} + sL + r}{G_v(s)G_i(s)e^{-1.5\mathrm{st}_s} + sCG_i(s)e^{-1.5\mathrm{st}_s} + LCs^2 + rCs + 1}. \tag{18}$$

According to the above analysis, virtual impedance technology takes advantage of virtual impedance $Z_v(s)$ to regulate internal impedance, from initial $Z(s)$ to $Z_n(s)$. Virtual impedance can be resistive [16], inductive [19], or resistive–inductive [20], the authors of [20] believe that resistive–inductive virtual impedance possesses the best control performance. However, inductive or resistive–inductive virtual impedance are not appropriate for the system.

Fig. 9 is the bode diagram of $Z_n(s)$ with inductive virtual impedance. Because the resonant controller is adopted, the impedance in the resonant frequency is very small. The inductive virtual impedance will change fundamental impedance characteristic and cannot keep resistive, makes resonant frequency shift and cannot keep 50 Hz, with frequency increasing, the harmonic impedance will gradually become larger, which is not beneficial to suppress harmonic, but inductive virtual impedance has little effect on the fundamental impedance amplitude, this is advantage of the inductive virtual impedance.

Fig. 10 is the bode diagram of $Z_n(s)$ with resistive virtual impedance. Comparing to inductive virtual impedance, resistive virtual impedance can make fundamental impedance remain resistive and keep resonant frequency at 50 Hz, but the defect of the resistive impedance is fundamental impedance that increases greatly and harmonic impedance does not get affected.

In fact, the objective of virtual impedance is to regulate harmonic impedance by increasing harmonic impedance appropriately, harmonic current sharing ability can be improved, and the fundamental impedance can be regulated by the droop method. Therefore, a high-pass filter (HPF) is introduced to resistive

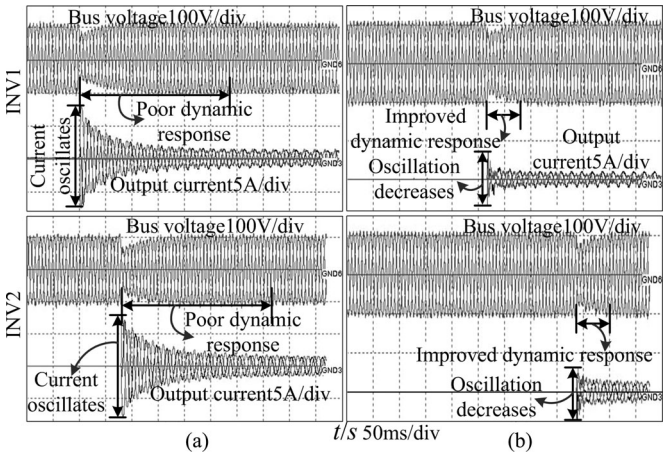

Fig. 21. Experimental result with the droop method. (a) Traditional method. (b) TWCADM.

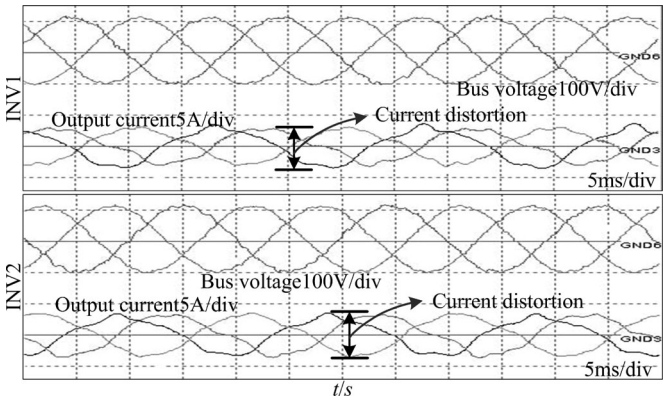

Fig. 22. Parallel system waveform with load.

virtual impedance

$$Z_v(s) = R_v \frac{s}{s + \omega_{\mathrm{hc}}} \tag{19}$$

where R_v is the resistive virtual impedance value, ω_{hc} is the cutoff frequency of HPF. The function of an HPF is to filter the fundamental component of the output current and so that

TABLE II
ACTUAL PARAMETERS

INV1		INV2	
Phase A inductance/mH	1.527	Phase A inductance/mH	1.541
Phase B inductance/mH	1.555	Phase B inductance/mH	1.57
Phase C inductance/mH	1.506	Phase C inductance/mH	1.513
Phase A parasitic resistance/Ω	0.027	Phase A parasitic resistance/Ω	0.028
Phase B parasitic resistance/Ω	0.03	Phase B parasitic resistance/Ω	0.031
Phase C parasitic resistance/Ω	0.027	Phase C parasitic resistance/Ω	0.026
Phase A capacitor/μC	21.5	Phase A capacitor/μC	20.5
Phase B capacitor/μC	20.3	Phase B capacitor/μC	20.5
Phase C capacitor/μC	19.4	Phase C capacitor/μC	21.4
Phase A sampling coefficient	99.7%	Phase A sampling coefficient	101%
Phase C sampling coefficient	100.2%	Phase B sampling coefficient	99.4%
Phase C sampling coefficient	100.3%	Phase C sampling coefficient	99.6%

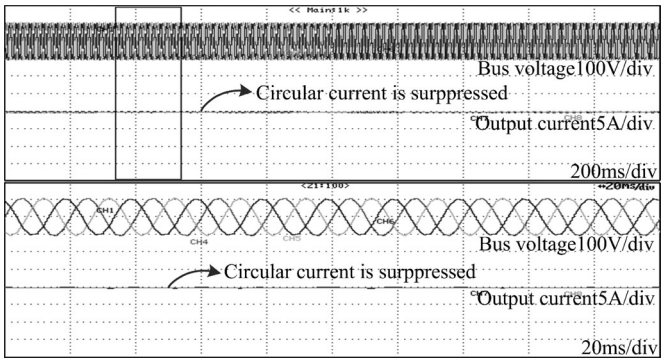

Fig. 23. Experimental result with no-load after increasing proportion droop coefficient and introducing voltage compensation strategy.

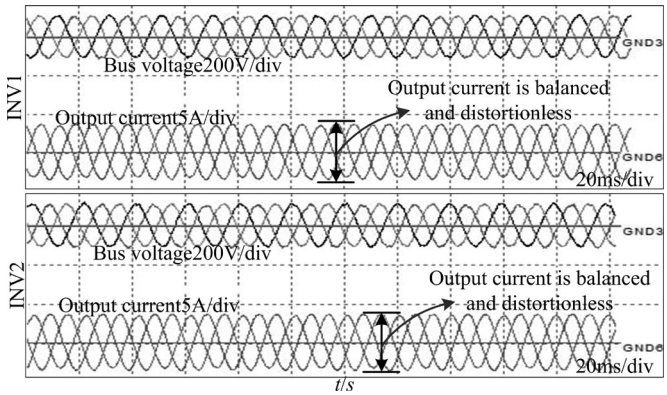

Fig. 24. Experimental result with load after increasing proportion droop coefficient and introducing voltage compensation strategy.

the fundamental impedance do not get affected, but the side effect of HPF is that the resonant frequency will shift.

As shown in Fig. 11, after introduction of an HPF, the offset of the resonant frequency increases with the increase of virtual impedance, and decreases with the increase of cutoff frequency. The essence of offset is the phase angle leading feature of HPF. For removing the offset of the resonant frequency, except for

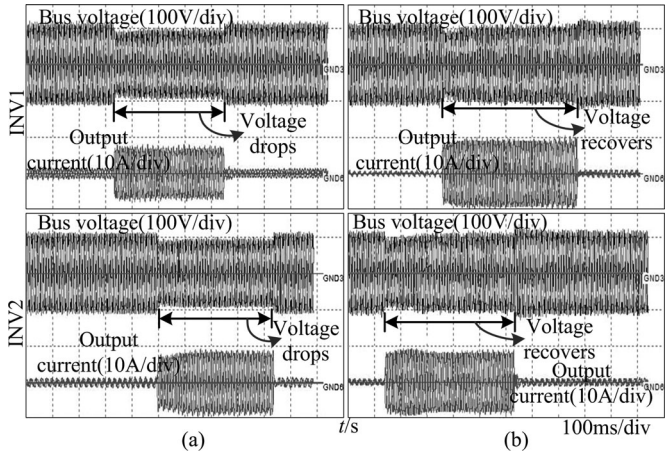

Fig. 25. Experimental results with pump load. (a) Without voltage compensation strategy. (b) With voltage compensation strategy.

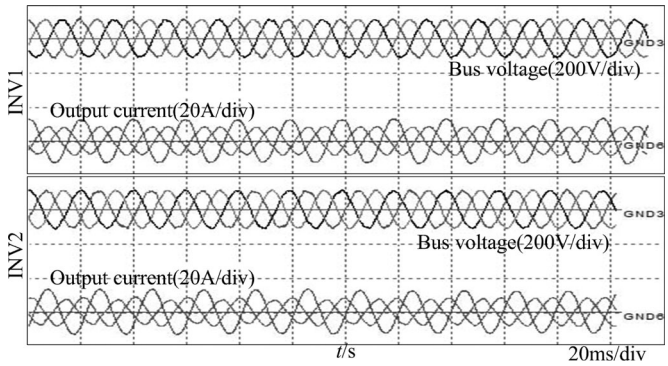

Fig. 26. Experimental result with unbalanced load.

selecting appropriate virtual impedance value and cutoff frequency, lagging feature of LPF is good choice for neutralizing the effect of HPF

$$Z_v(s) = R_v \frac{s}{s+\omega_{\rm hc}} \frac{1}{s+\omega_{\rm lc}} \tag{20}$$

where ω_{lc} is the cutoff frequency of LPF.

As can be seen from Fig. 12, combining effect of LPF and HPF, resistive virtual impedance has little effect on fundamental impedance; fundamental impedance still remains resistive and the resonant frequency of which does not shift. Virtual impedance affects only the harmonic impedance, the harmonic current can be shared by increasing harmonic impedance appropriately, which is smart and simple way to share the harmonic current.

Finally, the adopted total control strategy is shown in Fig. 13.

VI. SIMULATION

The simulation model is built by S-Function; simulation parameters are shown in Table I. Power is expressed by per unit value and 1 means 11375 kVA. Fig. 14(a) indicates that the parallel current are oscillating after paralleling in the traditional method, which means dynamic performance of the proportion droop method is poor. Fig. 14(b) indicates that dynamic

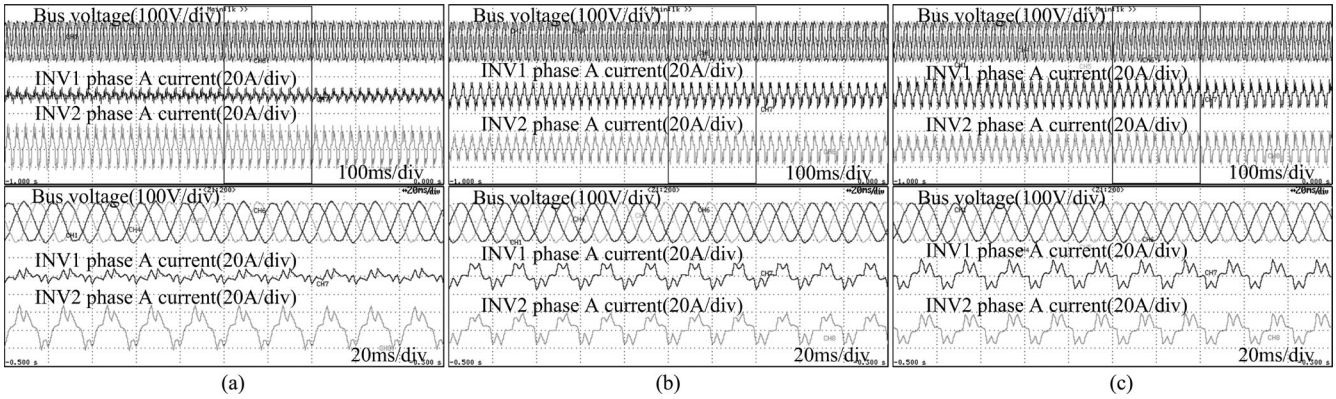

Fig. 27. Experimental results with nonlinear load. (a) With TWCADM. (b) With increasing proportion droop coefficient. (c) With virtual impedance technology.

performance is improved greatly, because the parallel current becomes stable and oscillation is suppressed rapidly.

Fig. 15 shows the simulation result of inconsistent parameters. Parameters of INV 1 includes: filter inductance is 1.7 mH, filter capacitor is 24μF, and sampling amplification coefficient is 1.02, and parameters of INV 2 includes: filter inductance is 1.3 mH, filter capacitor is 16μF, and sampling amplification coefficient is 0.98. For actual physical system, the above differences are possible to appear. The simulation result indicates that the output current cannot be shared with inconsistent parameters.

Fig. 16 indicates that increased proportion coefficient can share the output current again even if parameters are inconsistent (parameters of Fig. 16 are the same with Fig. 15), which sharp contrasts to unshared result of Fig. 15. However, increased proportion coefficient gives rise to one bad result, it is voltage drop, and voltage drop is more severe in single inverter, because increased proportion coefficient amounts to increased internal impedance.

Fig. 17 shows the simulation result of the voltage compensation strategy introduced into Fig. 16, the similarity between Fig. 16 and Fig. 17 is that the output current is always shared, the difference is that the amplitude of the bus voltage is almost recovered to the rated value, the disadvantage of increasing proportion coefficient has been overcome.

Fig. 18 shows the comparison of the simulation result under pump load: (a) is simulation result without voltage compensation strategy, (b) is simulation result with voltage compensation strategy; the output current in (a) and (b) are both shared, the bus voltage of (a) drops, however, because of the voltage compensation strategy, the voltage drop is compensated when pump load starts in (b).

Fig. 19 shows the simulation result with unbalanced load. Due to the improvement of control strategy, phase angel difference of each phase can always keep 120°, and the unbalanced current can be shared accurately.

Fig. 20 shows the simulation results with nonlinear load: (a) is without increasing the proportion droop coefficient, it indicates that the fundamental current and harmonic current are both unshared; (b) is the simulation result with increasing proportion droop coefficient, it indicates that the fundamental current can be shared and the harmonic current cannot be shared; (c) is the simulation result with virtual impedance technology and increasing proportion droop coefficient, it indicates that the fundamental current and harmonic current are both shared.

VII. Experimental Results

In this paper, a low-power experimental platform is built on the basis of Fig. 1; control system parameters and circuit parameters are shown in TABLE I. All waveforms are sampled by actual oscilloscope and virtual oscilloscope [22] through Ethernet, the rated voltage is reduced to 110 V (peak value) and the rated power of single inverter is 5 kVA.

Fig. 21 shows the experimental result with the droop method under no-load condition. Fig. 21(a) shows that the oscillating current generates after paralleling, which is the same with simulation. Because parameters of two inverters are inconsistent, the circular current always exists and cannot be eliminated. TWCADM makes for improving dynamic performance, as shown in Fig. 21(b); the oscillating current is reduced observably after TWCADM is introduced, which means dynamic performance is improved, but the circular current still cannot be eliminated by TWCADM.

Fig. 22 shows the parallel system waveform with load, three-phase output current distorts, it indicates that the circular current of each phase is different, which means parameters of each phase are also different. Actual parameters are listed in Table II, it indicates that inconstant parameters exist not only in each inverter but also in each phase.

Fig. 23 and Fig. 24 shows the experimental results after increasing the proportion droop coefficient and introducing the voltage compensation strategy, it can be seen from waveforms, regardless of load or no-load, the circular current is basically suppressed, the experimental result with load sharp contrasts to Fig. 22, three-phase current is balanced and undistorted.

Fig. 25 shows the experimental results with pump load, the voltage compensation strategy is employed in (b), the comparison between (a) and (b) indicates that voltage drops severely without voltage compensation strategy when pump load starts, which can be overcome by voltage compensation strategy, the voltage drop is almost suppressed at the moment of pump load starts, voltage drops for several periods but recovers rapidly.

Fig. 26 shows the experimental result with unbalanced load, load of phase A is $6.25\,\Omega$ and 12.34 mH, load of phase B is

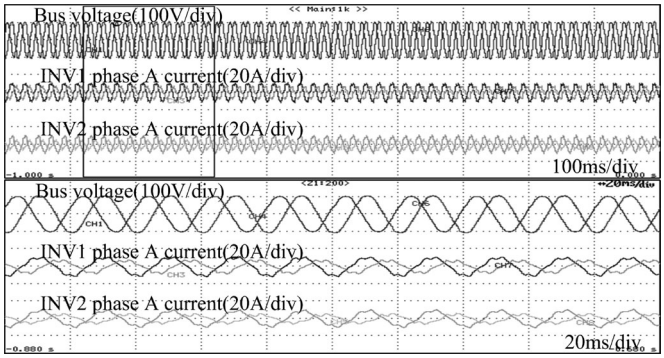

Fig. 28. Experimental result with unbalanced load and nonlinear load.

$12.5\,\Omega$ and 24.67 mH, load of phase C is $12.5\,\Omega$ and 24.67 mH; Fig. 28 indicates that phase angle difference of each phase can always keep 120° and unbalanced current is shared.

The experimental results with nonlinear load are shown in Fig. 27. Because of inconsistent parameters, (a) cannot share fundamental current and harmonic current. After increasing the proportion droop coefficient and introducing voltage compensation strategy in (b), the fundamental current can be shared rather than the harmonic current. With effect of virtual impedance technology, the fundamental current and harmonic current are both shared in (c).

Fig. 28 combines unbalanced load and nonlinear load, unbalanced load are 6.25, 12.5, and $12.5\,\Omega$, respectively, non-linear load is the rectifier diode with $100W$ and 80μF. Because of the proposed control strategy, unbalanced load and harmonic current are both shared.

VIII. Conclusion

The objective of this paper is to solve the problems in the auxiliary parallel system. This paper adopts the RDM to improve inherent contradiction between voltage regulation performance and power-sharing performance. In order to solve the problem of poor dynamic performance, this paper improves the power calculation method and introduces the whole cycle adaptive droop method, dynamic performance and stability of parallel system are both improved. With inconsistent parameters, the output current of the parallel system are difficult to be shared, this paper increases the proportion coefficient initiatively to improve current sharing performance, and introduces the voltage compensation strategy to recover the voltage drop caused by increasing the proportion coefficient. The load characteristic of the parallel auxiliary system is very complex, this paper employs the voltage compensation strategy to solve the voltage drop problem caused by the surge current when pump load starts, and utilizes the reactive power of the inverter to droop frequency and active power of each phase to droop amplitude, the unbalanced current caused by unbalanced load is shared, and introduces special deigned virtual impedance technology to share harmonic current caused by nonlinear load, therefore, the output current can be shared even if with complicated load.

References

[1] T. Iwade, S. Komiyama, Y. Tanimura, M. Yamanaka, M. Sakane, and K. Hirachi, "A novel small-scale UPS using a parallel redundant operation system," in *Proc. Telecommun. Energy Conf.*, Yokohama, Japan, 2003, pp. 480–484.

[2] L. Woo-Cheol, L. Taeck-Ki, L. Sang-Hoon, K. Kyung-Hwan, H. Dong-Seok, and S. In-Young, "A master and slave control strategy for parallel operation of three-phase UPS systems with different ratings," in *Proc. Appl. Power Electron. Conf. Expo.*, 2004, pp. 456–462.

[3] W. Tsai-Fu, C. Yu-Kai, and H. Yong-Heh, "3C strategy for inverters in parallel operation achieving an equal current distribution," *IEEE Trans. Ind. Electron.*, vol. 47, no. 2, pp. 273–281, Apr. 2000.

[4] Q. Shafiee, J. M. Guerrero, and J. C. Vasquez, "Distributed secondary control for islanded microgrids—A novel approach," *IEEE Trans. Power Electron.*, vol. 29, no. 2, pp. 1018–1031, Feb. 2014.

[5] H. Ming, H. Haibing, X. Yan, and J. M. Guerrero, "Multilayer control for inverters in parallel operation without intercommunications," *IEEE Trans. Power Electron.*, vol. 27, no. 8, pp. 3651–3663, Aug. 2012.

[6] H. Jiefeng, Z. Jianguo, D. G. Dorrell, and J. M. Guerrero, "Virtual flux droop method—A new control strategy of inverters in microgrids," *IEEE Trans. Power Electron.*, vol. 29, no. 9, pp. 4704–4711, Sep. 2014.

[7] J. C. Vasquez, R. A. Mastromauro, J. M. Guerrero, and M. Liserre, "Voltage support provided by a droop-controlled multifunctional inverter," *IEEE Trans. Ind. Electron.*, vol. 56, no. 11, pp. 4510–4519, Nov. 2009.

[8] S. V. Iyer, M. N. Belur, and M. C. Chandorkar, "A generalized computational method to determine stability of a multi-inverter microgrid," *IEEE Trans. Power Electron.*, vol. 25, no. 9, pp. 2420–2432, Sep. 2010.

[9] J. M. Guerrero, J. C. Vasquez, J. Matas, V. L. De, and M. Castilla, "Hierarchical control of droop-controlled AC and DC microgrids—A general approach toward standardization," *IEEE Trans. Ind. Electron.*, vol. 58, no. 1, pp. 158–172, Jan. 2011.

[10] C. Po-Tai, C. Chien-An, L. Tzung-Lin, and K. Shen-Yuan, "A cooperative imbalance compensation method for distributed-generation interface converters," *IEEE Trans. Ind. Appl.*, vol. 45, no. 2, pp. 805–815, Mar/Apr. 2009.

[11] J. M. Guerrero, J. Matas, V. L. De, M. Castilla, and J. Miret, "Wireless-control strategy for parallel operation of distributed-generation inverters," *IEEE Trans. Ind. Electron.*, vol. 53, no. 5, pp. 1461–1470, Oct. 2006.

[12] Q. Lei, F. Z. Peng, and S. T. Yang, "Multiloop control method for high-performance microgrid inverter through load voltage and current decoupling with only output voltage feedback," *IEEE Trans. Power Electron.*, vol. 26, no. 3, pp. 953–960, Mar. 2011.

[13] L. Corradini, P. Mattavelli, M. Corradin, and F. Polo, "Analysis of parallel operation of uninterruptible power supplies loaded through long wiring cables," *IEEE Trans. Power Electron.*, vol. 25, no. 4, pp. 1046–1054, Apr. 2010.

[14] K. Sedraoui, F. Fnaiech, and K. Al-Haddad, "Application of the instantaneous power with the symmetrical components theory to control unbalanced and non-sinusoidal three phase power system," in *Proc. Power Eng. Soc. General Meeting*, Tampa, FL, USA, 2007, pp. 1–6.

[15] A. Hasanzadeh, O. C. Onar, H. Mokhtari, and A. Khaligh, "A proportional-resonant controller-based wireless control strategy with a reduced number of sensors for parallel-operated UPSs," *IEEE Trans. Power Del.*, vol. 25, no. 1, pp. 468–478, Jan. 2010.

[16] D. De and V. Ramanarayanan, "Decentralized parallel operation of inverters sharing unbalanced and nonlinear loads," *IEEE Trans. Power Electron.*, vol. 25, no. 12, pp. 3015–3025, Dec. 2010.

[17] J. M. Guerrero, J. C. Vasquez, J. Matas, M. Castilla, and V. L. De, "Control strategy for flexible microgrid based on parallel line-interactive UPS systems," *IEEE Trans. Ind. Electron.*, vol. 56, no. 3, pp. 726–736, Mar. 2009.

[18] J. M. Guerrero, V. L. De, J. Matas, M. Castilla, and J. Miret, "A wireless controller to enhance dynamic performance of parallel inverters in distributed generation systems," *IEEE Trans. Power Electron.*, vol. 19, no. 5, pp. 1205–1213, Sep. 2004.

[19] J. M. Guerrero, L. GarciadeVicuna, J. Matas, M. Castilla, and J. Miret, "Output impedance design of parallel-connected UPS inverters with wireless load-sharing control," *IEEE Trans. Ind. Electron.*, vol. 52, no. 4, pp. 1126–1135, Aug. 2005.

[20] Y. Wei, C. Min, J. Matas, J. M. Guerrero, and Q. Zhao-Ming, "Design and analysis of the droop control method for parallel inverters considering the impact of the complex impedance on the power sharing," *IEEE Trans. Ind. Electron.*, vol. 58, no. 2, pp. 576–588, Feb. 2011.

[21] H. Deng, R. Oruganti, and D. Srinivasan, "A simple control method for high-performance UPS inverters through output-impedance reduction," *IEEE Trans. Ind. Electron.*, vol. 55, no. 2, pp. 888–898, Feb. 2008.
[22] W. Lei, L. Zhigang, Z. Gang, and Z. Leiting, "A multi-channel distributed monitoring platform based on Ethernet and virtual instrument technology," in *Proc. Int. Conf. Electron. Meas. Instrum.*, 2009, pp. 4–579.

Jie Chen was born in Zhejiang, China, in 1986. He received the B.S. and Ph.D. degrees in electrical engineering and automation from Beijing Jiaotong University, Beijing, China, in 2008 and 2013 respectively.

Since 2013, he has been a Postdoctoral Researcher with Beijing Jiaotong University, and also with the Institute of Electrical Engineering, Chinese Academy of Sciences, Beijing. He is currently a Visiting Scholar of WEMPEC in the University of Madison, Madison, WI, USA. His research interests include variable frequency drive, rail transportation traction control, and inverter parallel control.

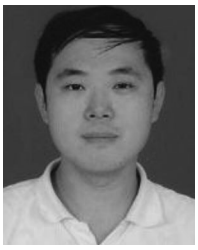

Lei Wang was born in Shandong, China, in 1982. He received the B.S. degree from the Institute of Information and Control Engineering, University of Petroleum, Shandong, China, in 2005, and the Ph.D. degree from the Institute of Electrical Engineering, Beijing Jiaotong University, Beijing, China, in 2010.

From 2010 to 2012, he was a Postdoctoral Researcher of traffic transportation engineering at the Institute of Electrical Engineering, Chinese Academy of Science, Beijing. Since 2012, he has been a Faculty Member of power electronics and ac drives with the Department of Electrical Engineering, Beijing Jiaotong University, Beijing. His research interests include power supply configuration, power-saving technology, traction control, auxiliary power conversion, communication network, and net-based monitoring.

Lijun Diao (S'05–M'10) was born in Guangdong, China, in 1980. He received the bachelor's degree in electrical engineering and automation, and the Ph.D. degree in power electronics and ac drives from Beijing Jiaotong University, Beijing, China, in 2003 and 2008, respectively.

After receiving the Ph.D. degree, he was a Traffic Transportation Engineer at Beijing Jiaotong University between 2008 and 2010, where since 2008, he has been a Faculty of power electronics and ac drives with the Department of Electrical Engineering. His research interests include power electronics, power semiconductor and application, and rail transportation traction control and safety.

Huiqing Du was born in Hebei, China, in 1988. He received the B.S. degree in electrical engineering from Beijing Jiaotong University, Beijing, China, in 2011, where he is currently working toward the Ph.D. degree.

His research interests include auxiliary power conversion control, battery charger.

Zhigang Liu was born in Shandong, China, in 1961. He received the bachelor's, master's, and Ph.D. degrees in electric drive for locomotives from Beijing Jiaotong University, Beijing, China, in 1986, 1990, and 1994, respectively.

He is a Vice Chairman of the China Electrotechnical Society Rail Transport Electrical Technical Committee, and he is also an evaluation expert of several national key plans.

He is currently a Full Professor at Beijing Jiaotong University. In the recent years, he presided over a number of national key scientific research projects and achieved fruitful results in the field of rail transit power supply, traction control, safety prediction and control, etc. He published a book on power electronics and spent several months as a Visiting Scholar in the U.S. and Canada. His teaching activities and research interests include power electronics circuit and system, rail transportation traction control and safety, etc.